

Effect of neutron irradiation on the microstructure of tungsten



M. Klimenkov^{a,*}, U. Jäntschi^a, M. Rieth^a, H.C. Schneider^a, D.E.J. Armstrong^b, J. Gibson^b, S.G. Roberts^b

^a Karlsruhe Institute of Technology (KIT), Institute for Applied Materials, 76021 Karlsruhe, Germany

^b University of Oxford, Department of Materials, Oxford, UK

ARTICLE INFO

Article history:

Available online 14 October 2016

Keywords:

Tungsten

Neutron irradiation

Microstructure

Transmutation

ABSTRACT

Two grades of pure tungsten, single and polycrystalline, were irradiated for 282 days in the HFR reactor, Petten, at 900 °C to an average damage level of 1.6 dpa. Each grade of tungsten was investigated using the transmission electron microscope (TEM) to assess the effect of neutron irradiation on tungsten microstructure. Investigations revealed the formation of faceted cavities, whose diameter varies from 4 to 14 nm in both materials. The cavities are homogeneously distributed only inside single crystalline tungsten. The local distribution of cavities in polycrystalline tungsten is strongly influenced by grain boundaries. The number densities of cavities were measured to be $4 \times 10^{21} \text{ m}^{-3}$ for polycrystalline and $2.5 \times 10^{21} \text{ m}^{-3}$ for single crystalline tungsten. This corresponds to volumetric densities of 0.45% and 0.33% respectively. High-resolution transmission electron microscopy (HRTEM) revealed that faces of cavities are oriented in (110) plane. Analytical investigations showed precipitation of rhenium and osmium produced by a transmutation reaction around cavities and at grain boundaries.

© 2016 The Authors. Published by Elsevier Ltd.

This is an open access article under the CC BY-NC-ND license

(<http://creativecommons.org/licenses/by-nc-nd/4.0/>).

1. Introduction

Tungsten (W) is considered to be the most promising choice for the plasma-facing component of fusion reactors because of its favourable properties, such as a high melting point, high sputtering resistivity, and high temperature strength. Due to the high melting temperature of W, even for the very high expected operating temperature for W in fusion reactors significant irradiation-induced damage is expected [1,2].

Characterisation of microstructural and mechanical properties of neutron-irradiated W was covered by several publications in the past [3–5]. In most studies W was irradiated with doses of less than 1.5 dpa in the 400–800 °C temperature range. An extensive microstructural study and review of irradiated pure W and W-Re alloys was performed by Hasegawa et al. [4]. The results published in numerous papers are summarised in the diagram which shows defect formation depending on radiation dose and temperature [4]. Analysing this Hasegawa-diagram can be concluded that irradiation of pure W at 800 °C to doses higher as 1 dpa leads to the formation of cavities only. Microstructures with both dislocation loops and cavities were observed only at irradiation doses down to 0.5 dpa.

Current results relating to the W microstructure after 1.6 dpa irradiation at 900 °C are beyond the temperature and radiation ranges of Hasegawa-diagram [4] and, hence, can be considered a complement to the already published results.

Irradiation in the sub-dpa ranges does not lead to a significant accumulation of rhenium (Re) or osmium (Os). In former studies W-Re or W-Re-Os alloys were neutron-irradiated in order to simulate the influence of transmutation-induced elements on the microstructure and mechanical properties [3,5,6]. As was shown, the presence of Re influences the formation of cavities and contributes to the increased hardening of material.

Single crystalline and polycrystalline W specimens were subjected to neutron irradiation in the High Flux Test Reactor (HFR) up to a dose of 1.6 dpa at 900 °C in order to evaluate microstructural changes, including formation of radiation-induced cavities as well as precipitation of Re and Os produced by a complex chain of transmutation reactions. Imaging of the two-dimensional distribution of these elements allows conclusions to be drawn with respect to their influence on the microstructure under real working conditions.

2. Experimental

The single crystalline and polycrystalline samples of commercially pure W from Metals Crystal and Oxides Limited, Cambridge,

* Corresponding author. Fax: +49 721 608 24567.

E-mail address: michael.klimenkov@kit.edu (M. Klimenkov).

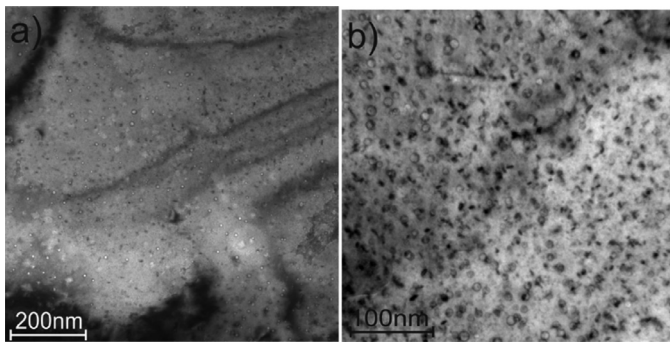


Fig. 1. TEM images of single crystal material obtained with different magnifications.

UK were irradiated for 208 days positioned in two different locations in the High Flux Reactor (HFR), Petten, at 900 °C. The materials were also used in previous studies published in refs. [7–9]. The total neutron flux was $6.8 \times 10^{18} \text{ m}^{-2} \text{ s}^{-1}$ ($3.2 \times 10^{18} \text{ m}^{-2} \text{ s}^{-1}$, $E < 0.1 \text{ MeV}$) for the first location (148 full power days) and $6.6 \times 10^{18} \text{ m}^{-2} \text{ s}^{-1}$ ($3.2 \times 10^{18} \text{ m}^{-2} \text{ s}^{-1}$, $E < 0.1 \text{ MeV}$) for the second location (60 full power days). The samples were positioned next to another experiment with very strong neutron absorption properties, so that material was exposed to a lower than normal for HFR fraction of thermal neutrons. Inventory simulation was performed with FISPACT-II [10] of pure W taking into consideration detailed irradiation schedule and neutron spectrum.

The Re and Os concentrations in irradiated W were calculated to 1.4% and 0.1% respectively. The calculated Re concentration (C_{Re}) is in the good agreement with 1.2–1.4 wt.% values from quantitative energy dispersive x-ray (EDX) measurements in TEM performed by comparison of $W\text{-}L_{\alpha}$ (8.40 keV) and $Re\text{-}L_{\alpha}$ (8.65 keV) line intensities (I) using $C_{\text{Re}} = C_W \times (I_{\text{Re}}/I_W)$ equation. The estimated statistical error of 20% for the measurement of $Re\text{-}L_{\alpha}$ line intensity makes the consideration of Cliff-Lorimer $k_{W\text{Re}} = 0.987$ factor for quantification not useful. The radiation damage was calculated to 1.6 dpa in the W using displacement threshold of $E_d = 55 \text{ eV}$.

Post-irradiation microstructural examination of both materials was performed in the Fusion Materials Laboratory (FML) at KIT. Thin foils for TEM investigations were prepared using the FIB technique and deposited on a molybdenum grid. The flash polishing ($12 \text{ V} \times 50 \text{ ms}$) was applied to remove surface radiation damage after FIB preparation. TEM characterisation was performed using an FEI Tecnai 20 FEG microscope with an accelerating voltage of 200 kV, a scanning unit for performing scanning TEM (STEM) with a high-angle annular dark field (HAADF) detector, and an EDAX energy dispersive x-ray (EDX) detector for elemental analysis. The analytical investigations by STEM-EDX were made with a beam size of 1.0–1.5 nm.

3. Results

The TEM images show the formation of nano-sized faceted cavities in both poly-crystalline and single crystal materials (Figs. 1, 2). The images were obtained from the grains with crystallographic orientation far from low indexed zone axes near to two-beam conditions. Such orientation in the bright field mode makes possible contrast-rich imaging of structural defects. The cavities and needle shaped Re-rich precipitates with typical size $3 \text{ nm} \times 15 \text{ nm}$ are homogeneously distributed in the single crystal material (Fig. 1a,b). The Re-rich precipitates have approximately the same number density as cavities. The spatial distribution of cavities in polycrystalline material is influenced by grain boundaries. A 20 nm thick zone denuded of cavities was observed adjacent to both sides of grain boundaries. No cavity has been detected direct at the grain

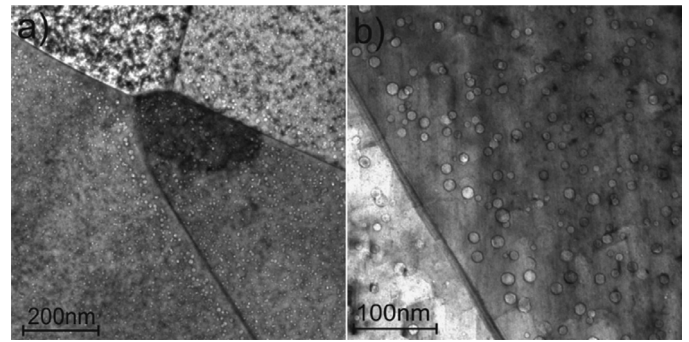


Fig. 2. TEM images of polycrystalline material obtained with different magnifications.

boundaries (Fig. 2a, b). The histograms which reveal the size distribution of cavities in both materials are shown in Fig. 3. Their diameter varies from 3 to 14 nm with an average value 5–5.5 nm. The fraction of cavities with diameter larger than 10 nm is higher in the polycrystalline than in single crystal material. The largest cavities have been formed in the area near to the grain boundary. The number densities of cavities are measured to be $4 \times 10^{21} \text{ m}^{-3}$ for the polycrystalline material and $2.5 \times 10^{21} \text{ m}^{-3}$ for the single crystalline material. This corresponds to volumetric densities of 0.45% for the polycrystalline material and 0.38% for the single crystal material, respectively. The cavities with sizes larger than 10 nm have been formed in the area near to the grain boundaries in polycrystalline material. The thickness of TEM foils was measured to 45 nm in Fig. 1a and 110 nm in Fig. 2a. This difference in the thicknesses is the reason for visible much higher number density of cavities in polycrystalline material by comparison Figs. 1a and 2a.

The cavities often show a faceted structure which reflects their orientation in the matrix. Fig. 4 shows the high-resolution TEM (HRTEM) micrograph of a 6 nm cavity in a grain oriented with [110] zone axis (a) together with the corresponding fast Fourier transformation (FFT) image (b). The imaged atomic planes of (110) and (200) types with $d_{110} = 2.26 \text{ nm}$ and $d_{200} = 1.62 \text{ nm}$ correspond to the cubic structure of W. These results show that the void's facets are preferably formed in the 110 plane. The faceted shape is well visible in cavities which diameter is larger than 5 nm, whereas cavities with diameter smaller than 5 nm rather exhibit a round shape in TEM images.

In addition to the formation of structural defects or cavities, the production of transmutation elements, such as Re and Os, was observed after neutron irradiation of W [3]. The EDX measurements obtained from the area of several microns show that originally pure W contains 1.3% Re and $> 0.5\%$ Os after irradiation in HFR. This value is in the good agreement with calculations. Irradiation-induced precipitation of these elements may influence the mechanical properties and microstructure of W, as previously observed in ion irradiated W-Re and W-Re-Os alloys [11,12]. To identify the Re distribution, two-dimensional EDX analysis with a fine electron probe, whose diameter was approximately 1 nm, was performed (Figs. 5, 6). The cavities are visible in HAADF images as dark spots (Figs. 5a, 6a). The scanned area in the polycrystalline material, which is marked by a square, includes a triple point at the grain boundaries (Fig. 5). The W and Re maps demonstrate that Re is preferably located at structural defects, such as grain boundaries and around cavities. The quantitative analysis of EDX spectra shows that Re concentration at the grain boundary can be estimated to be in the 12%–18% range. In some cavities a Re-rich circle can be recognised. This circle has been formed around each, even the smallest, void. The density of Re-rich precipitates in the single crystal material is approximately 2 times higher than that of

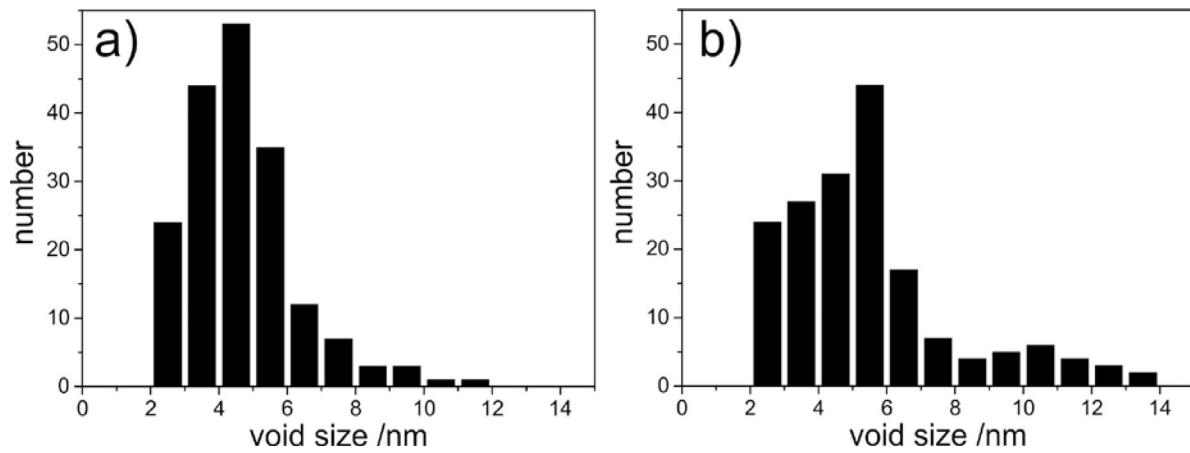


Fig. 3. Size distribution histograms of cavities in single crystal (a) and polycrystalline (b) materials.

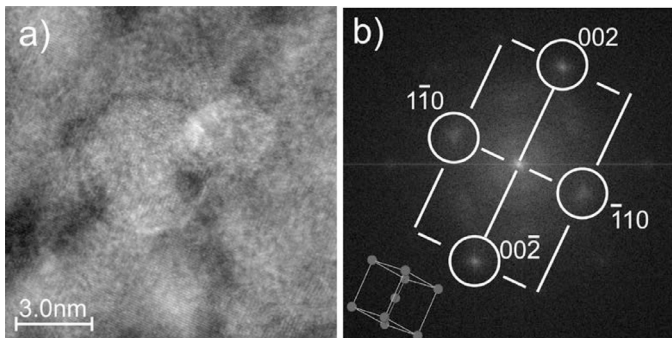


Fig. 4. HRTEM image of a void (a) corresponding FFT analysis (b).

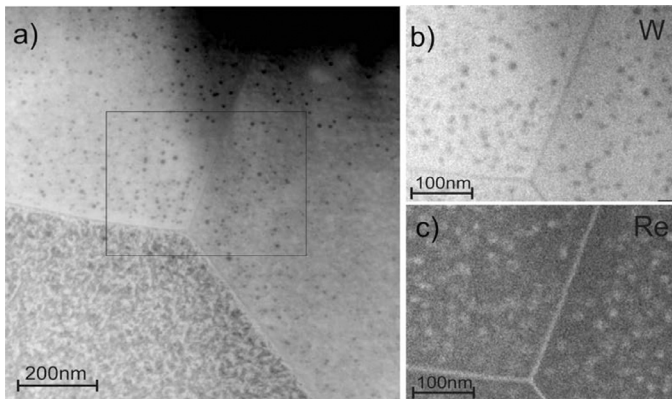


Fig. 5. Two-dimensional elemental mapping of polycrystalline material. HAADF image of the investigated area (a) as well as W (b) and Re (c) maps.

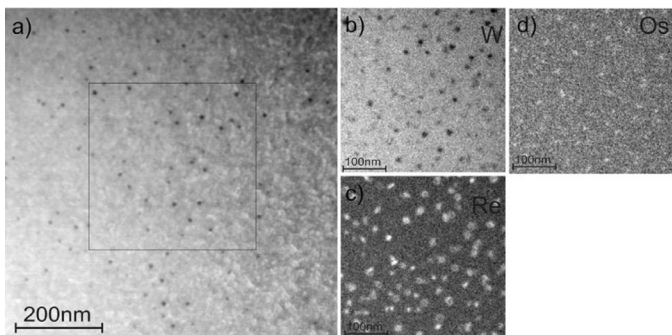


Fig. 6. Two-dimensional elemental mapping of single crystalline material. HAADF image of the investigated area (a) as well as W (b), Re (c) and Os (d) maps.

cavities. In the area analysed in Fig. 6, 43 cavities and 90 Re-rich precipitates were counted. The dark points in the W map indicate the distribution of not only cavities, but also of W-deficiencies in Re-rich precipitates.

4. Discussion

Recently, numerous publications covered the characterization of neutron-irradiated W or W-Re alloys [2–6]. Based on the experimental microstructure data presented in ref. [4], a diagram was drawn, which shows defect formation as a function of damage dose and irradiation temperature. The diagram covers the temperature range from 350 °C to 800 °C and damage doses of up to 1.5 dpa. The data in this diagram show that damage structures can be subdivided into cavities and loops-and-cavities areas. The cavities seem to be main damage structures for W. The concentrations of dislocation loops detected in W irradiated to a dose of less than 1 dpa is 5–10 times smaller than concentration of cavities in the same material [13]. The increase of radiation dose to more than 1 dpa leads to the formation of cavities only. In our study, where the specimens were irradiated to a dose of 1.6 dpa, the formation of loops was not observed. Generally, the cavities found in irradiated W are smaller than 10 nm. The average size varied in the range from 3 nm to 7 nm [6]. The average size of cavities in the present publication was measured to be 5 nm (Fig. 3). This is similar to the average value of 4.7 nm measured in materials irradiated at 750° and 1.5 dpa [6]. It can be concluded that the increase of irradiation temperature to 900 °C at the dose of 1.6 dpa and does not influence the size of cavities in W significantly.

The number density of cavities, however, varies by 2 orders of magnitude mostly as a function of the irradiation temperature. Irradiation at temperatures below 750 °C leads to the formation of cavities with number densities from $1 \times 10^{23} \text{ m}^{-3}$ to $5 \times 10^{23} \text{ m}^{-3}$ [7]. At the temperature of 800 °C, cavities are formed with $8 \times 10^{21} \text{ m}^{-3}$ number density [12]. Irradiation at 900 °C and 1.6 dpa as performed within the framework of the present study results in a number density value of $2.5 \times 10^{21} \text{ m}^{-3}$ for a single crystal and $4 \times 10^{21} \text{ m}^{-3}$ for a polycrystalline material. These results show that number densities of cavities tend to decrease with increased irradiation temperature.

The local differences in the number density of cavities were obtained in the area near the grain boundaries. A zone of 15–25 nm with only few cavities was formed around the grain boundaries (Fig. 7). Just outside of this zone has been formed a 100–120 nm thick void-concentrated region. The number density of cavities in this region is approximately two times higher than that in the inner grains. Such variations of number density were also observed

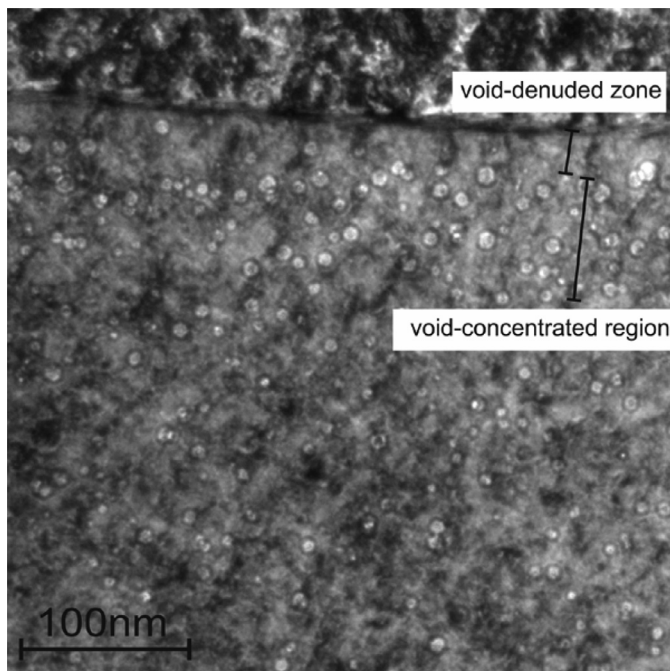


Fig. 7. TEM image of cavities in the region near a grain boundary.

in W irradiated at 800 °C/0.98 dpa [3,13]. The explanation of such cavities distribution given in by Fukuda et.al [3] is that, the grain boundary acts as a strong sink for radiation induced point defects (i.e., vacancies and interstitials). This prevents formation of cavities in the area next the grain boundaries and benefits the formation of void-denuded layer. However, the diffusivity of interstitials is faster than that of vacancies. As a result, a “void peak” zone was formed outside of the void-denuded layer. A presence of Re could also suppress formation of cavities. It was shown that their number density is significantly lower in W-Re alloy than in pure W [12]. As the grain boundaries serve also as a sink for Re atoms its concentration in the region near grain boundaries could be reduced. This could accelerate the formation of cavities near grain boundaries. However, this effect cannot be reliably quantified. Possibly influence of 1.4% wt. Re is lower compare to the other effects.

Two-dimensional distributions of Re show that this element preferably precipitates on structural defects, such as cavities, and in polycrystalline material on the grain boundaries (Fig. 6). In the polycrystalline material Re was found to precipitate only on the grain boundaries or around the cavities, whereas single crystal material contains many Re-rich precipitates which are not connected with a void (Fig. 6). Formation of Re-rich sigma- or chi- phases with elongated shapes was not detected. The void/Re-precipitate ratio is approximately 1 in polycrystalline material, whereas in single crystal W this ratio is about 0.50 (Fig. 6). The precipitation of Re on the grain boundaries probably plays an important role for the differences between polycrystalline and single crystal W. This precipitation reduces Re concentration inside grains in polycrystalline material and, consequently, weakens its effect on the microstructure. As in was shown in ref. [14], the formation of cavities was significantly suppressed in W-Re alloys as compared to pure W. In general, the experimental data collected during the last 7 years show that the microstructure of neutron-irradiated W depends not only on temperature, but also on Re-Os concentration. The fact that Re concentration increases during irradiation at a rate that depends on the neutron spectrum allows only general suggestions to be made with respect to its effect on the

microstructure. Thus far-reaching conclusions by comparison of our data with irradiated W-Re alloys are not yet possible. This has important consequences for understanding how the microstructural evolution W will occur in a true fusion neutron spectrum, much more work is needed on quantifying the synergistic effects minor transmutation elements have on the formation of clusters and precipitates.

5. Conclusions

A microstructural characterization of polycrystalline and single crystal W irradiated at 900 °C to 1.6 dpa was performed. The results can be summarized as follows:

- The formation of radiation-induced cavities with sizes mainly less than 10 nm was observed. The number density of cavities was measured to be $2.5 \times 10^{21} \text{ m}^{-3}$ in the single crystal and $4 \times 10^{21} \text{ m}^{-3}$ in the polycrystalline material. The void-denuded zone and void peak area were observed around the grains.
- The 1.4% Re produced by the transmutation reaction is subject to radiation-induced precipitation at the grain boundaries and around the cavities. Formation of Re rich precipitates was observed in single crystal material.
- The observed differences in the number densities of cavities in polycrystalline and single crystal W might be caused by the lower Re concentration due to adhesion on grain boundaries in the polycrystalline material. The formation of Re-rich particles with a round shape was detected in the single crystal material. These particles were formed independently of cavities.

Acknowledgements

This study was supported financially by the EPSRC under Programme grant EP/H018921/1. J. Gibson is grateful for support from CCFE for an EPSRC I-CASE award. D.E.J. Armstrong is grateful for the funding provided by a Royal Academy of Engineering Research Fellowship. The Neutron irradiation was performed as part of the EXTRE-MAT FP6 project.

This work has been carried out within the framework of the EUROfusion Consortium and has received funding from the Euratom research and training programme 2014–2018 under grant agreement No. 633053. The views and opinions expressed herein do not necessarily reflect those of the European Commission.

References

- [1] H. Bolt, V. Barabash, W. Krauss, J. Linke, R. Neu, S. Suzuki, N. Yoshida, J. Nucl. Mater. 329–333 (2004) 66–73.
- [2] M.R. Gilbert, J.-Ch. Sublet, Nucl. Fusion 51 (2011) 043005.
- [3] M. Fukuda, A. Hasegawa, T. Tanno, Sh. Nogami, H. Kurishita, J. Nucl. Mater. 442 (2013) S273–S276.
- [4] A. Hasegawa, M. Fukuda, Sh. Nogami, K. Yabuuchi, Fus. Eng. Des. 89 (2014) 1568–1572.
- [5] A. Hasegawa, M. Fukuda, T. Tanno, K. Yabuuchi, Mater. Trans. 54 (2013) 466–471.
- [6] T. Tanno, M. Fukuda, S. Nogami, A. Hasegawa, Mater. Trans. 52 (2011) 1447–1451.
- [7] A. Giannattasio, S.G. Roberts, Philos. Mag. 87 (2007) 2589–2598.
- [8] A. Giannattasio, Z. Yao, E. Tarleton, S.G. Roberts, Philos. Mag. 90 (2010) 3947–3959.
- [9] J. Gibson, S.G. Roberts, D. Armstrong, Mater. Sci. Eng.: A 625 (2015) 380–384.
- [10] M.R. Gilbert, L.W. Packer, J.-Ch. Sublet, R.A. Forrest, Nuclear Sci. Eng. 177 (2014) 291–306.
- [11] D.E.J. Armstrong, X. Yi, E.A. Marquis, S.G. Roberts, J. Nuclear Mater. 432 (2013) 428–433.
- [12] A. Xu, C. Beck, D.E.J. Armstrong, K. Rajan, G.D.W. Smith, P.A.J. Bagot, Acta Mater. 87 (2015) 121–127.
- [13] M. Fukuda, K. Yabuuchi, S. Nogami, A. Hasegawa, T. Tanaka, J. Nucl. Mater. 455 (2014) 460–463.
- [14] T. Tanno, A. Hasegawa, J.-C. He, M. Fujiwara, S. Nogami, M. Satou, T. Shishido, K. Abe, Mater. Trans. 48 (2007) 2399–2402.